Science Immunology
AAAS

immunology.sciencemag.org/cgi/content/full/4/36/eaaw1217/DC1

Supplementary Materials for

PD-1^{hi} CD8^{+} resident memory T cells balance immunity and fibrotic sequelae

Zheng Wang, Shaohua Wang, Nick P. Goplen, Chaofan Li, In Su Cheon, Qigang Dai, Su Huang, Jinjun Shan, Chaoyu Ma, Zhenqing Ye, Min Xiang, Andrew H. Limper, Eva-Carmona Porquera, Jacob E. Kohlmeier, Mark H. Kaplan, Nu Zhang, Aaron J. Johnson, Robert Vassallo, Jie Sun*

*Corresponding author. Email: sun.jie@mayo.edu

Published 14 June 2019, *Sci. Immunol.* **4**, eaaw1217 (2019)
DOI: 10.1126/sciimmunol.aaw1217

The PDF file includes:

Other Supplementary Material for this manuscript includes the following:

(available at immunology.sciencemag.org/cgi/content/full/4/36/eaaw1217/DC1)

Table S1 (Microsoft Excel format). Raw data.

Fig. S1

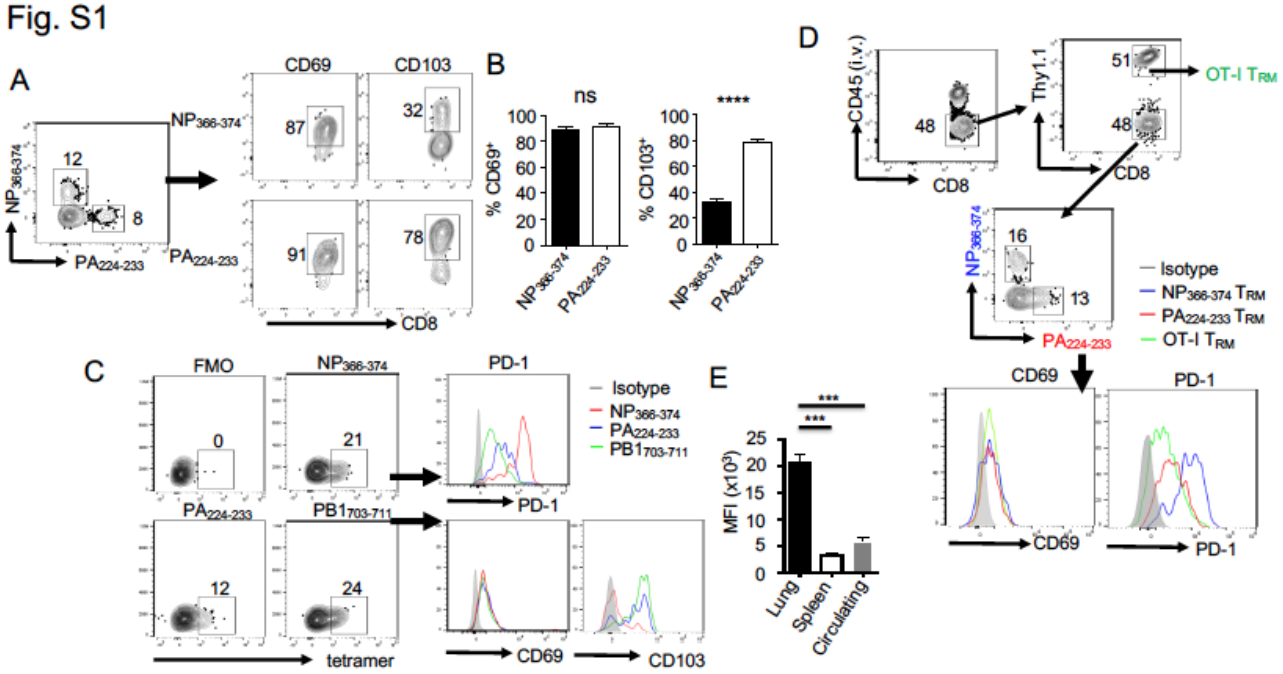

Fig. S1 Epitope-specific expression of CD103 and PD-1 on T_{RM}. WT mice were infected with PR8. **(A).** Expression of CD69 and CD103 on lung $NP_{366-374}$ or $PA_{224-233}$ T_{RM} cells at 40 d.p.i. **(B).** Percentages of $CD69^+$ or $CD103^+$ cells on lung $NP_{366-374}$ or $PA_{224-233}$ T_{RM}. (C). CD69, CD103 or PD-1 expression on lung $NP_{366-374}$, $PA_{224-233}$ or $PB1_{703-711}$ tetramer$^+$ cells at 40 d.p.i. (D) WT mice were transferred with OVA-specific Thy1.1$^+$ OT-I T cells and then infected with recombinant PR8-OVA. T_{RM} cells were examined at 45 d.p.i. PD-1 and CD69 expression by OT-I T_{RM}, endogenous $NP_{366-374}$ or $PA_{224-233}$ T_{RM} cells is depicted. (E). MFI of PD-1 expression on $NP_{366-374}$ lung T_{RM}, spleen memory and lung circulating (labeled with i.v. Ab) memory T cells. Data are mean ± SD, n.s., not significant. $^*P < 0.05$, $^{**}P < 0.01$, $^{***}P < 0.001$, unpaired two-tailed *t* test or One-way ANOVA with Tukey multiple comparison test.

Fig. S2

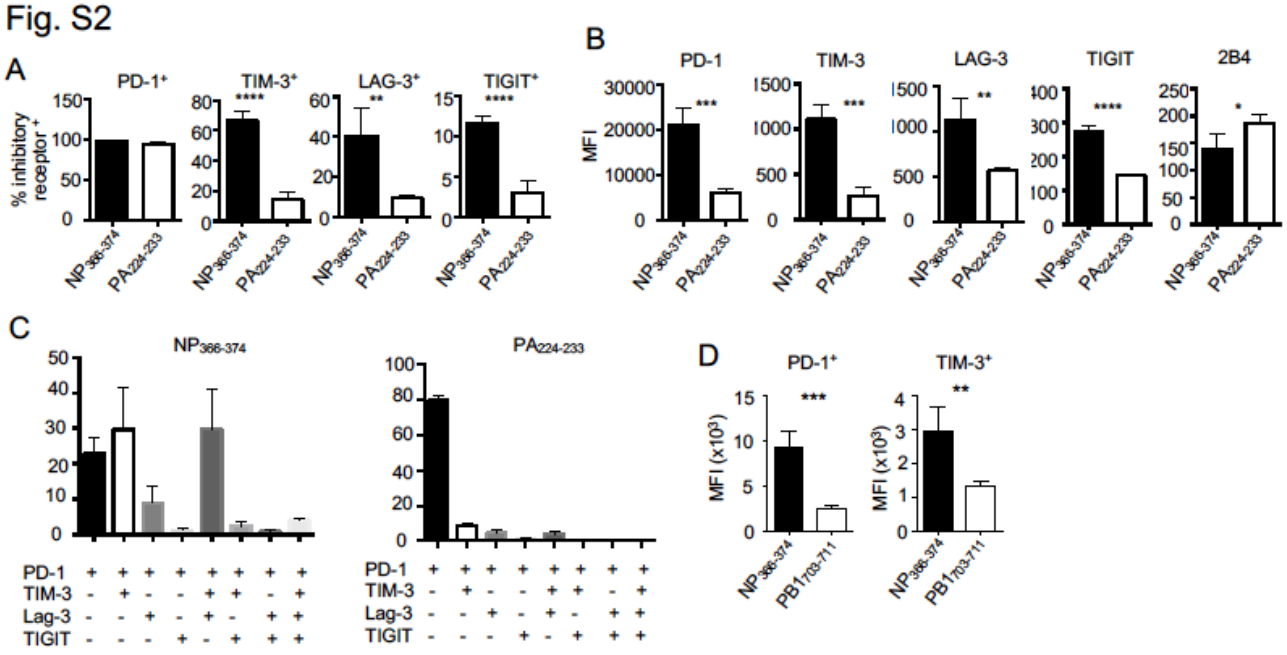

Fig. S2 Epitope-specific expression of inhibitory receptors on T_{RM}. WT mice were infected with PR8 and T_{RM} cells were examined at 40 d.p.i. (A). Quantification of % inhibitory receptor expression on $NP_{366-374}$ or $PA_{224-233}$ T_{RM} cells. (B). MFI of individual inhibitory receptor expression on $NP_{366-374}$ or $PA_{224-233}$ T_{RM} cells. (C). Simultaneous expression of multiple inhibitory receptors (PD-1, LAG-3, Tim-3 and TIGIT) on $NP_{366-374}$ or $PA_{224-233}$ T_{RM} cells. (D). MFI of PD-1 or TIM-3 expression on $NP_{366-374}$ or $PB1_{703-711}$ T_{RM} cells. Data are mean ± SD, n.s., not significant. $^{*}P < 0.05$, $^{**}P < 0.01$, $^{***}P < 0.001$, unpaired two-tailed *t* test.

Fig. S3

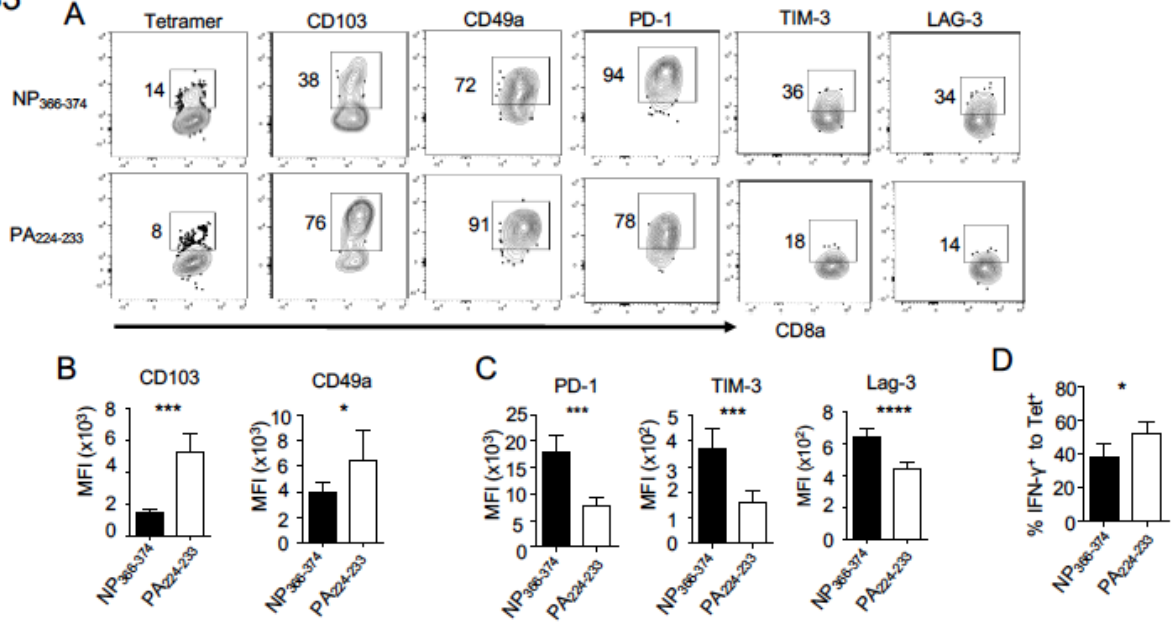

Fig. S3 Exhausted-like T_{RM} cells are present in X31 influenza model. (A-C). WT mice were infected with influenza X31 strain and T_{RM} cells were examined at 40 d.p.i. (A). Representative plots of tetramer staining and CD103, CD49a, PD-1, TIM-3 or LAG-3 staining on $NP_{366-374}$ or $PA_{224-233}$ T_{RM} cells. (B). MFI of CD103 or CD49a expression on lung $NP_{366-374}$ or $PA_{224-233}$ T_{RM} cells. (C). MFI of inhibitory receptors expression on lung $NP_{366-374}$ or $PA_{224-233}$ T_{RM} cells. (D). WT mice were infected with PR8. T_{RM} cells were examined following $NP_{366-374}$ or $PA_{224-233}$ peptide stimulation at 40 d.p.i. % IFN-γ^+ cells relative to $NP_{366-374}$ or $PA_{224-233}$-specific T_{RM} cells (tetramer$^+$ cells). Representative of two experiments. Data are mean ± SD, n.s., not significant. *P < 0.05, **P < 0.01, ***P < 0.001, unpaired two-tailed t test.

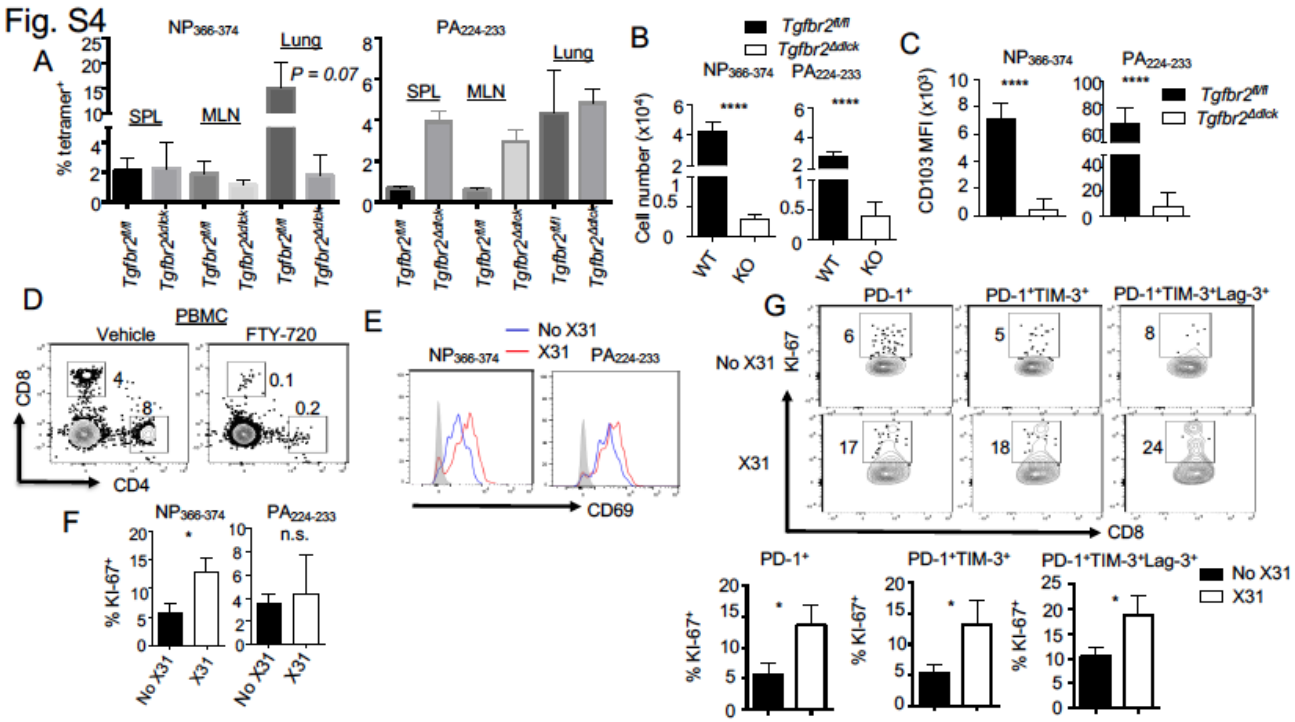

Fig. S4 Exhausted-like T_{RM} cells respond effectively to recall *in situ*. (A-C). Control (*Tgfbr2*$^{fl/fl}$) or *Tgfbr2*$^{\Delta dlck}$ mice were infected with PR8. (A). % of $NP_{366-374}$ or $PA_{224-233}$ –specific T cells in the spleen (SPL), draining mediastinal lymph nodes (MLN) or the lungs at 9 d.p.i. (B). $NP_{366-374}$ or $PA_{224-233}$ T_{RM} cells were enumerated at 42 d.p.i. (C) CD103 MFI on $NP_{366-374}$ or $PA_{224-233}$ T_{RM} cells at 42 d.p.i. (D-G). WT mice were infected with PR8 and re-challenged with X31 at day 40 in the presence of FTY-720 to block T cell migration from lymphoid organs. Mice were sacrificed two days later for analysis. (D). % CD8 or CD4 T cells in PBMCs 24 hours following Vehicle or FTY-720 treatment. (E). CD69 expression on lung $NP_{366-374}$ or $PA_{224-233}$ cells. (F). % KI-67$^+$ cells in lung $NP_{366-374}$ or $PA_{224-233}$ cells. (G). Representative plots (up) and quantification (down) of percentages of KI-67$^+$ cells in indicated inhibitory receptor(s)$^+$ lung $NP_{366-374}$ cells. Representative of two to three experiments except in A. Data are mean ± SD, n.s., not significant. *P < 0.05, **P < 0.01, ***P < 0.001, unpaired two-tailed t test.

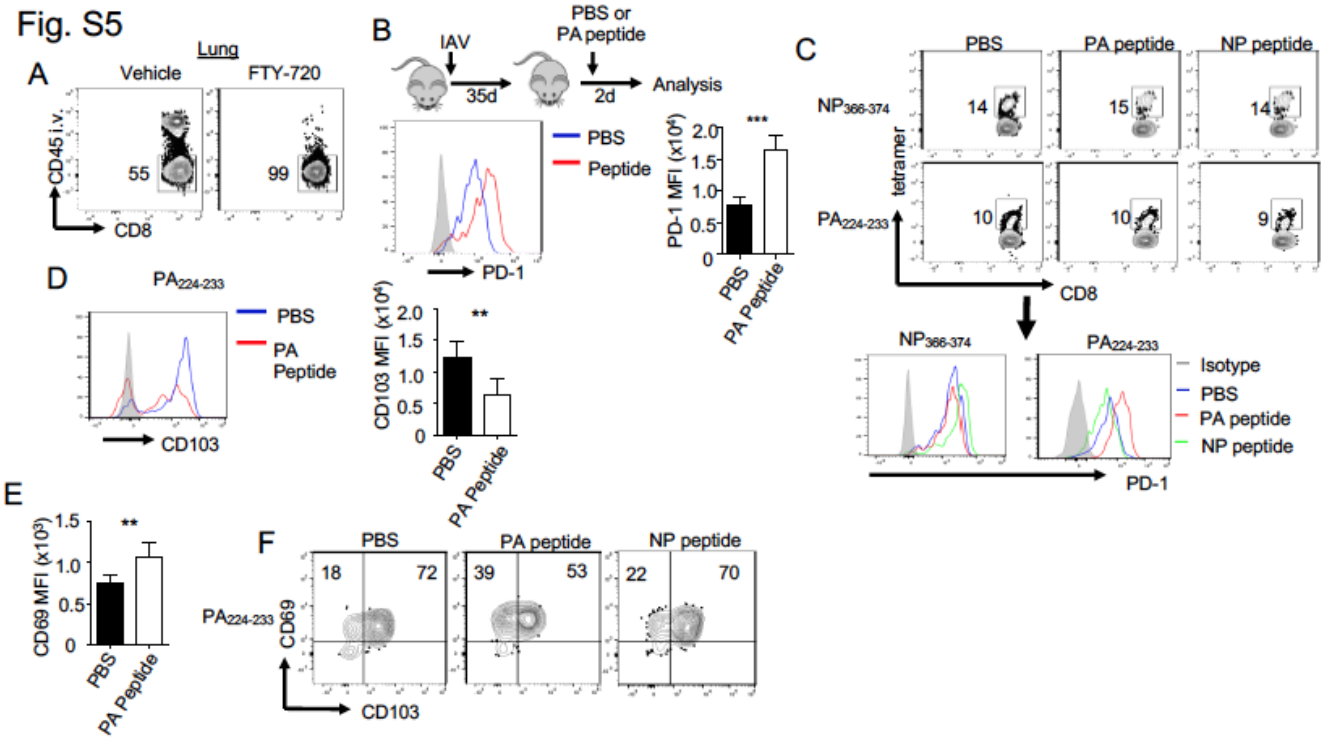

Fig. S5 Cognate peptide inoculation directly promotes PD-1 expression on $PA_{224-233}$ T_{RM} cells. (A). WT mice were infected with PR8 and received vehicle or FTY-720 daily starting at 21 d.p.i. Mice were sacrificed at 40 d.p.i. % of i.v. CD45 Ab^+ cells in lung $CD8^+$ T cells is depicting. (B-F). WT mice were infected with PR8. (B). Schematic of experimental design, representative histogram (left) and quantification (right) of PD-1 expression on $PA_{224-233}$ T_{RM} cells following PBS or $PA_{224-233}$(PA) peptide innoculation. (C). PD-1 expression on $PA_{224-233}$ or $NP_{366-374}$ T_{RM} following PBS, PA or NP peptide inoculation. (D). Representative histogram (left) and quantification (right) of CD103 expression on $PA_{224-233}$ T_{RM} cells. (E). CD69 expression on $PA_{224-233}$ T_{RM} cells. (F). Representative plots of CD69/CD103 expression on $PA_{224-233}$ T_{RM} cells with or without peptide inoculation. Representative of two or three experiments. Data are mean ± SD, *P < 0.05, **P < 0.01, ***P < 0.001, unpaired two-tailed t test.

Fig. S6

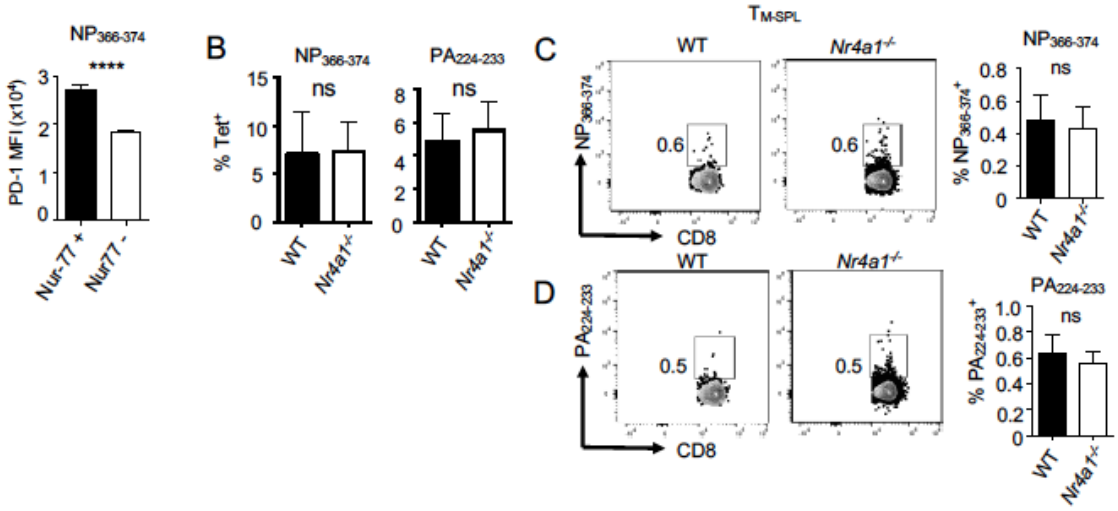

Fig. S6 Nur77 (*Nr4a1*) is required for the induction and/or maintenance of exhausted-like T_{RM} cells. (A). Nur77-GFP mice were infected with PR8. PD-1 MFI of Nur-77-GFP$^+$ and Nur-77-GFP$^-$ $NP_{366-374}$ T_{RM} cells at 40 d.p.i.(B-D). WT and *Nr4a1*$^{-/-}$ mixed bone marrow chimeric mice were constructed and infected with PR8. (B). Percentages of $NP_{366-374}$ or $PA_{224-233}$ tetramer$^+$ cells in the PBMCs at 12 d.p.i. (C). Representative plots (left) and quantification (right) of percentages of $NP_{366-374}$ spleen memory T cells at 40 d.p.i. (D). Representative plots (left) and quantification (right) of percentages of $PA_{224-233}$ spleen memory T cells. Representative of two experiments at 40 d.p.i. Data are mean ± SD, n.s., not significant. *P < 0.05, **P < 0.01, ***P < 0.001, unpaired two-tailed t test.

Fig. S7

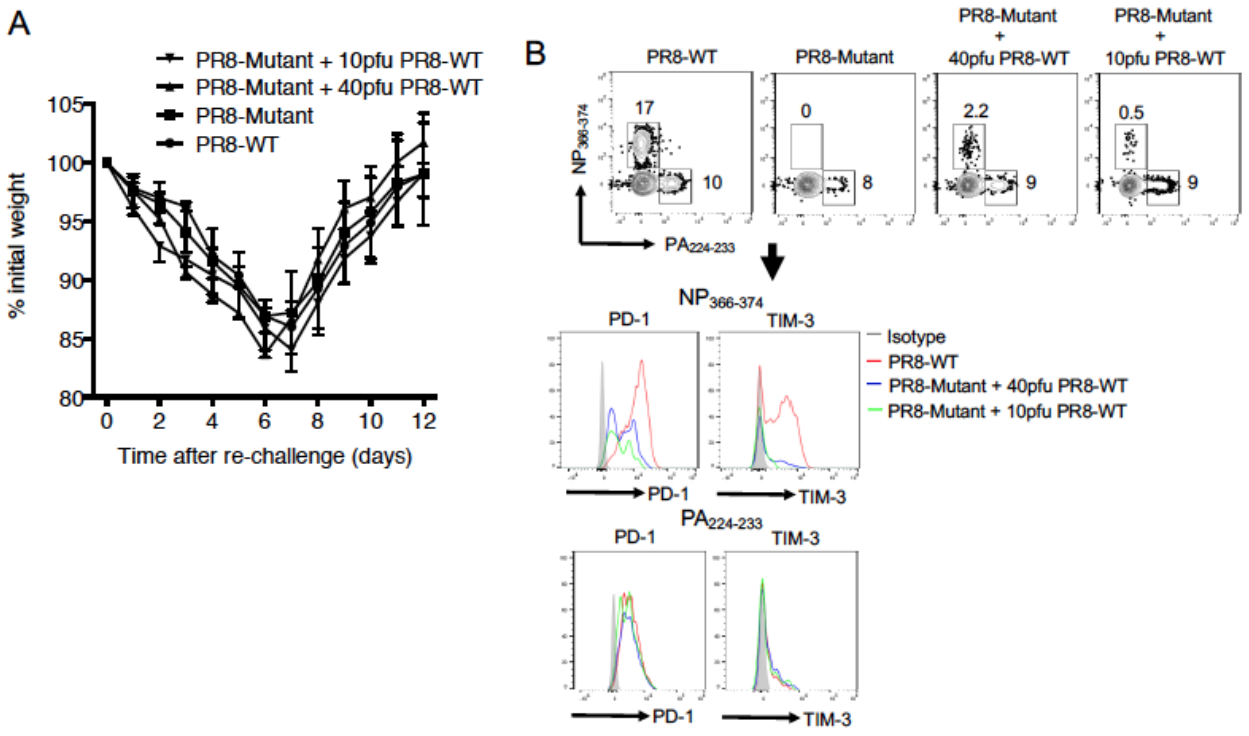

Fig. S7 Limiting NP antigen dose decreases the "exhaustion" phenotype. WT mice were infected with WT PR8 virus, PR8 NP mutant virus, PR8 NP mutant virus mixed with 10 pfu WT PR8 virus or PR8 NP mutant virus mixed with 40 pfu WT PR8 virus. (A) Host morbidity (% of initial weight) following infection. (B) PD-1 and TIM-3 expression on $NP_{366-374}$ or $PA_{224-233}$ T_{RM} at 40 d.p.i.

Fig. S8

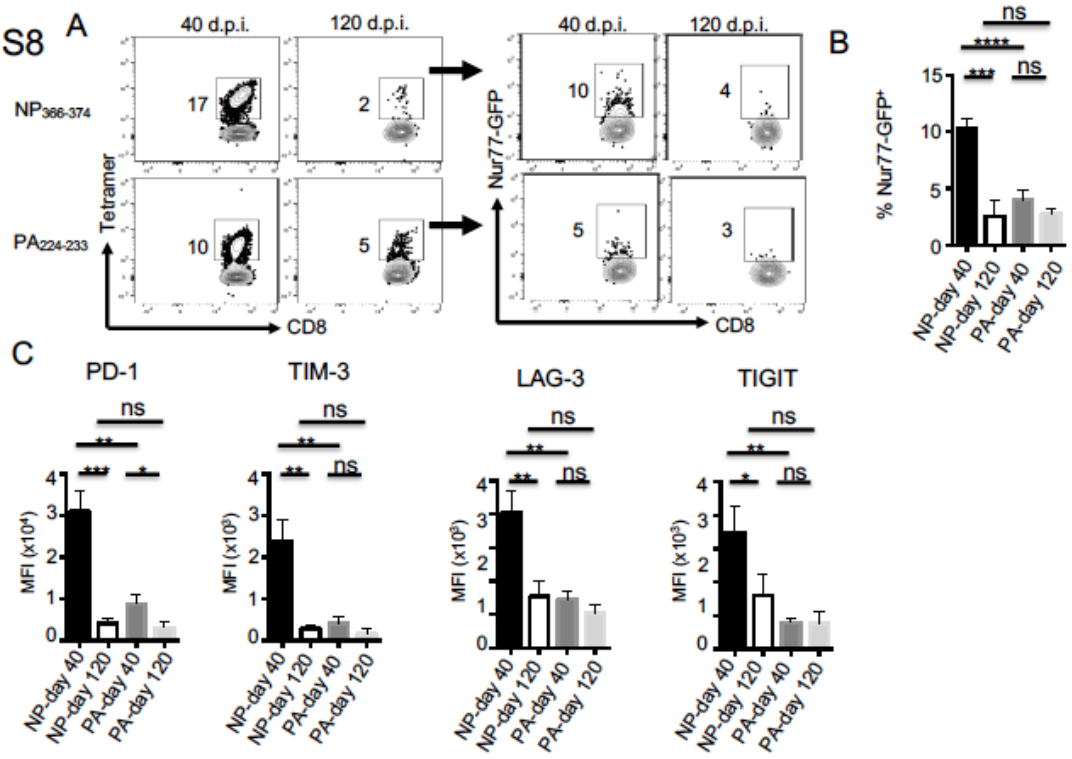

Fig. S8 TCR signaling and inhibitory receptor expression on exhausted-like T_{RM} cells are lost 4 months after infection. (A-C). Nur77-GFP mice were infected with PR8 and T_{RM} cells were analyzed at 40 or 120 d.p.i. (A). Representative plots of Nur77-GFP expression in $NP_{366-374}$ T_{RM} cells at 40 or 120 d.p.i. (B). Quantification of percentages of Nur77-GFP$^+$ cells in $NP_{366-374}$ or $PA_{224-233}$ T_{RM} cells at 40 or 120 d.p.i. (C). MFI of inhibitory receptors expression on $NP_{366-374}$ or $PA_{224-233}$ T_{RM} cells at 40 or 120 d.p.i. Representative of three experiments. Data are mean ± SD, n.s., not significant. *P < 0.05, **P < 0.01, ***P < 0.001, unpaired two-tailed *t* test or One-way ANOVA with Tukey multiple comparison test.

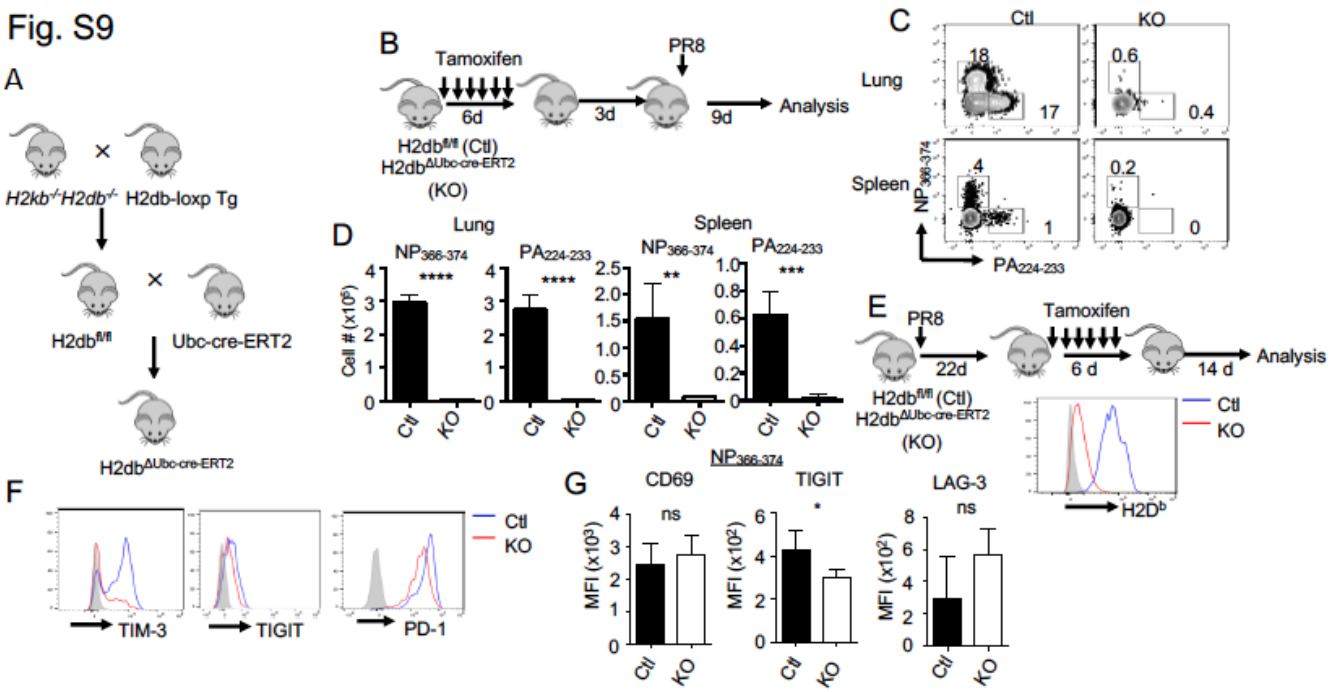

Fig. S9 Persistent MHC-I engagement maintains exhausted-like T_{RM} cell phenotypes and cells. (A). Strategy of generation of $H2db^{\Delta Ubc\text{-}cre\text{-}ERT2}$ (KO) mice. H2db-loxp transgenic mice were first bred to MHC-I KO (*H2kb*$^{-/-}$*H2db*$^{-/-}$) mice to generate *H2db*$^{fl/fl}$ mice. These animals were then crossed to Ubc-creERT2 transgenic mice to generate Ubc-creERT2/*H2db*$^{fl/fl}$ double transgenic mice in MHC-I-deficient background (*H2db*$^{\Delta Ubc\text{-}creERT2}$) . (B-D). Control or $H2db^{\Delta Ubc\text{-}cre\text{-}ERT2}$ (KO) mice were treated with tamoxifen and then infected with PR8. (B) Schematics of experimental design. (c). Representative plots of $NP_{366\text{-}374}$ or $PA_{224\text{-}233}$ specific T cells in lung or spleen $CD8^+$ T cells at 9 d.p.i. (D) Total cell numbers of $NP_{366\text{-}374}$ or $PA_{224\text{-}233}$ specific T cells in lung or spleen at 9 d.p.i. (E). Schematic of experimental design and representative histogram of H-$2D^b$ expression in lung $CD45^+$ cells of control and KO mice 72 hours following last tamoxifen injection. (F). Representative histogram of PD-1, TIM-3 or TIGIT expression on $NP_{366\text{-}374}$ T_{RM} cells at 42 d.p.i. (G). Quantification of MFI of CD69, TIGIT or LAG-3 expression on $NP_{366\text{-}374}$ T_{RM} cells at 42 d.p.i. Data are mean ± SD, n.s., not significant. *P < 0.05, **P < 0.01, ***P < 0.001, unpaired two-tailed t test.

Fig. S10

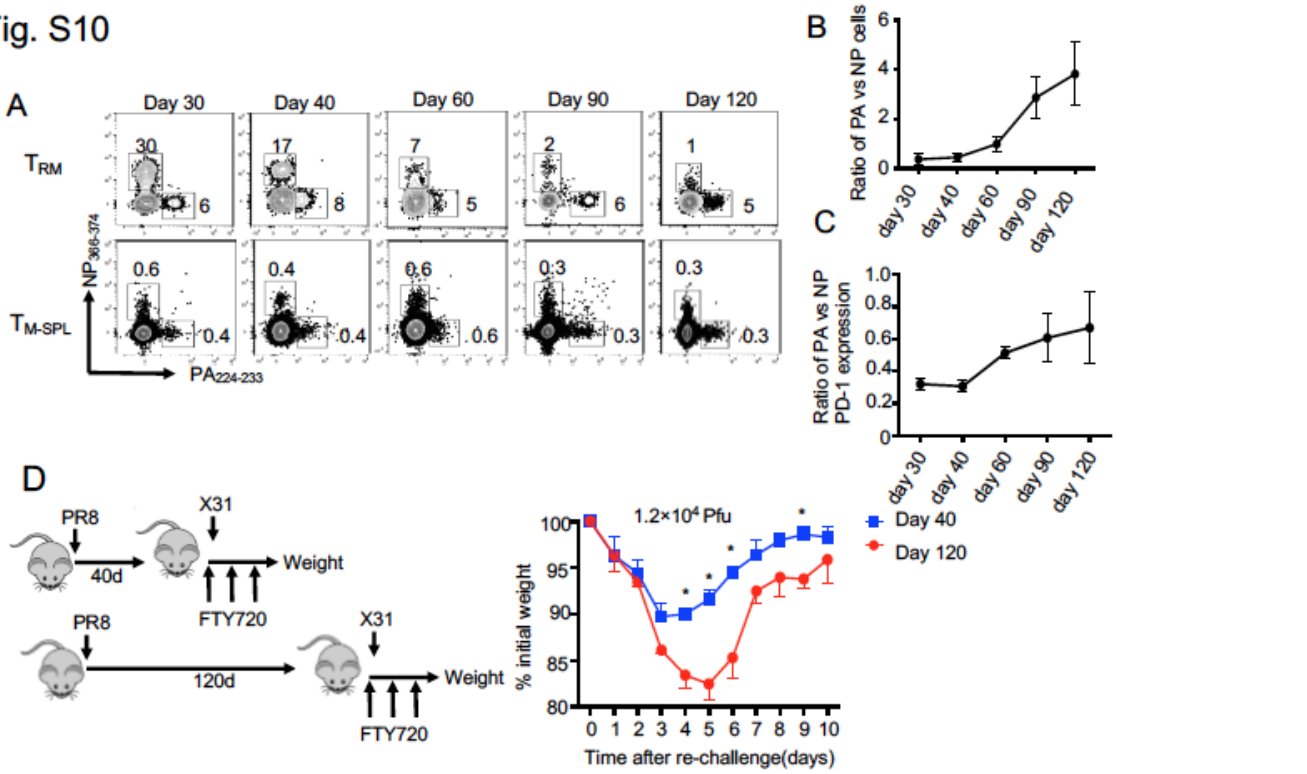

Fig. S10 $NP_{366-374}$ T_{RM} cells, PD-1 expression and heterologous protection are lost over time. (A-C). WT mice were infected with PR8 and T_{RM} cells were analyzed at indicated d.p.i. (A). Representative plots of percentage of $NP_{366-374}$ and $PA_{224-233}$ T_{RM} cells or spleen memory T cells at indicated d.p.i. (B). Kinetics of ratio of % $PA_{224-233}$ to % $NP_{366-374}$ T_{RM} at indicated d.p.i.. (C). Kinetics of ratio of $PA_{224-233}$ T_{RM} PD-1 expression to $NP_{366-374}$ T_{RM} PD-1 expression at indicated d.p.i. (D). WT mice were infected with PR8. Mice were re-challenged with X-31 (1.2×10^4 pfu/mouse) in the present of FTY-720 at 40 and 120 d.p.i. Mouse weight loss (% initial weight) was determined daily following re-challenge. Representative of two experiments. Data are mean ± SD, *P < 0.05, **P < 0.01, ***P < 0.001, unpaired two-tailed t test.

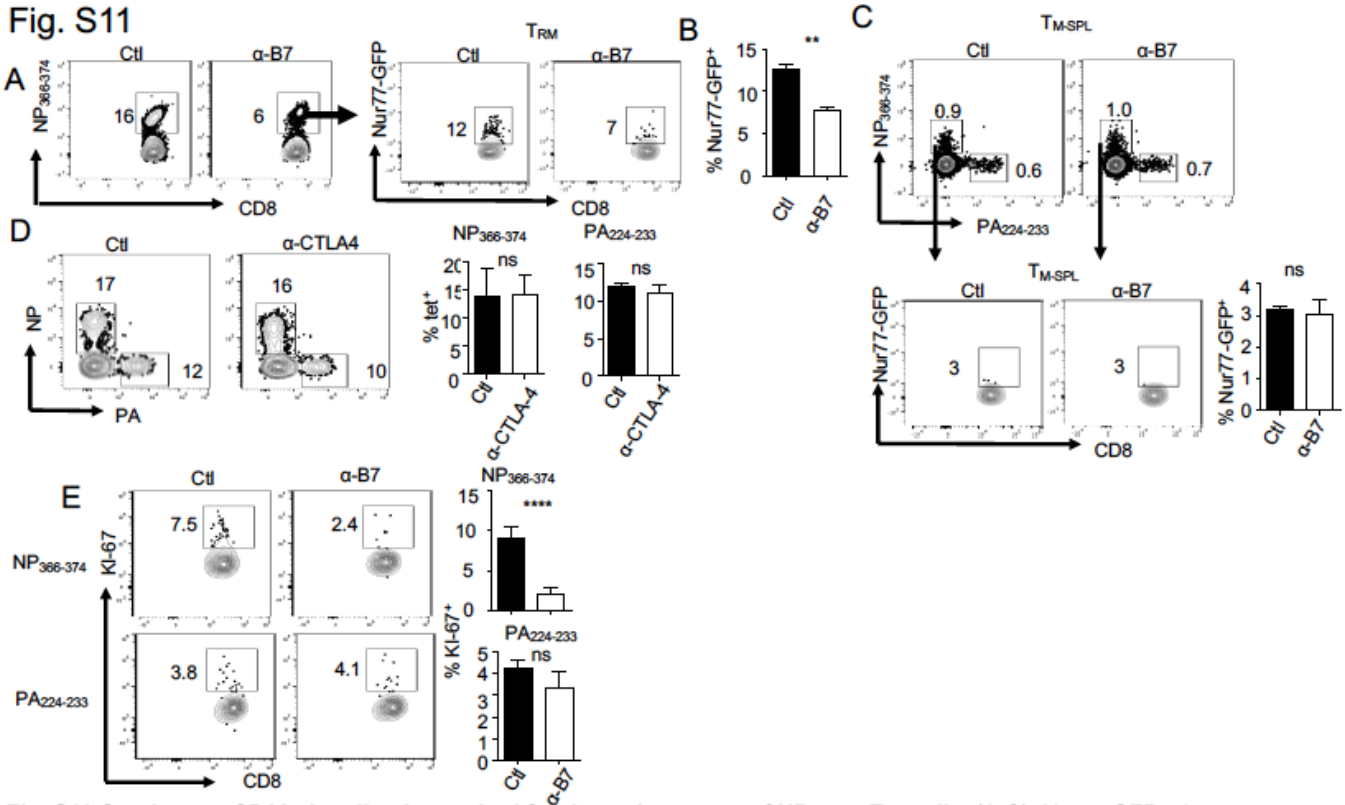

Fig. S11 Continuous CD28 signaling is required for the maintenance of $NP_{366-374}$ T_{RM} cells. (A-C). Nur77-GFP mice were infected with PR8 and treated with control Ab or α-B7 starting at day 21 p.i. T_{RM} cells were analyzed at 42 d.p.i. Representative plots (A) and percentages (B) of Nur77-GFP$^+$ cells in $NP_{366-374}$ T_{RM} cells. (C). Representative plots (left) and percentages (right) of Nur77-GFP$^+$ cells in $NP_{366-374}$ spleen memory T cells. (D). WT mice were infected with PR8 and treated with control Ab or α-CTLA-4 starting at day 21 p.i.. Representative plots (left) and % (right) of $NP_{366-374}$ or $PA_{224-233}$ T_{RM} cells at 42 d.p.i. (E) WT mice were infected with PR8 and treated with control Ab or α-B7 starting at day 21 p.i. Representative plots (left) and % of KI-67$^+$ (right) cells in $NP_{366-374}$ or $PA_{224-233}$ T_{RM} cells. Representative of two to three experiments except (A). Data are mean ± SD, n.s., not significant. *P < 0.05, **P < 0.01, ***P < 0.001, unpaired two-tailed t test.

Fig. S12

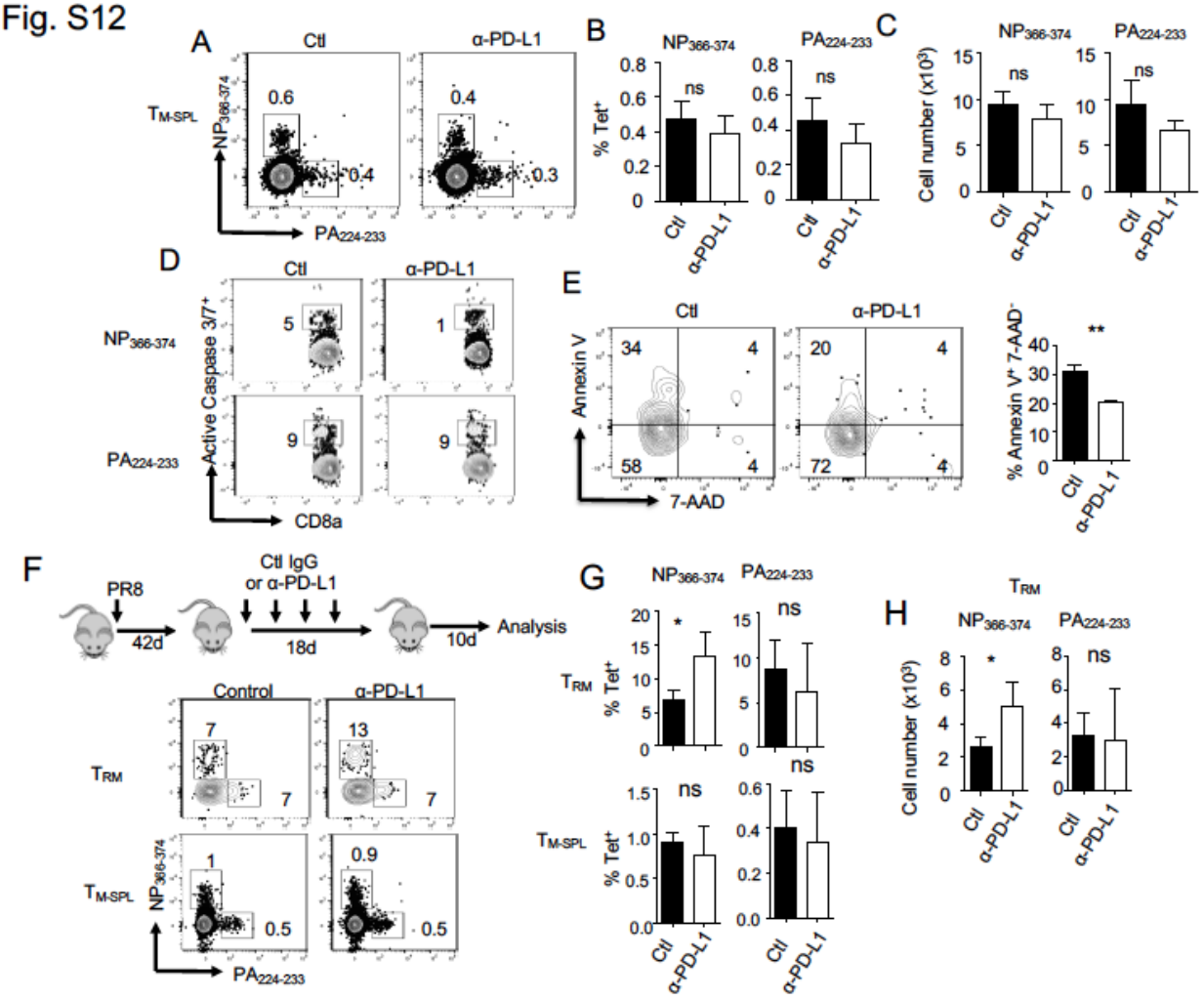

Fig. S12 PD-L1 blockade promotes exhausted-like T_{RM} cell survival and CD103 expression. (A-E). WT mice were infected with PR8 and treated with control Ab or α-PD-L1 starting at day 21 p.i. T_{RM} cells were analyzed at 40 d.p.i. (A). Representative plots of % $NP_{366-374}$ or $PA_{224-233}$ in total CD8 T cells in the spleen. (B). Quantification of % $NP_{366-374}$ or $PA_{224-233}$ in splenic CD8 T cells. (C). Quantification of cell numbers of $NP_{366-374}$ or $PA_{224-233}$ spleen memory T cells. (D). Representative plots of active Caspase 3/7$^+$ cells in $NP_{366-374}$ or $PA_{224-233}$ T_{RM} with or without late PD-L1 blockade. (E). Representative plots of Annexin V/7-AAD expression (left) and quantification (right) of Annexin V$^+$ cells in $NP_{366-374}$ T_{RM} with or without late PD-L1 blockade.
(F-H). WT mice were infected with PR8. Mice were treated with control or α-PD-L1 starting at 42 d.p.i till 60 d.p.i.as indicated (F). (F). Representative plots of $NP_{366-374}$ or $PA_{224-233}$ T_{RM} frequencies in resident CD8$^+$ T cells at 70 d.p.i. (G). % of $NP_{366-374}$ or $PA_{224-233}$ T_{RM} or T_{M-SPL} in lung or splenic CD8 T cells at 70 d.p.i. (H). Numbers of $NP_{366-374}$ or $PA_{224-233}$ T_{RM} at 70 d.p.i. Representative of three to four experiments except (F-H). Data are mean ± SD, n.s., not significant. *P < 0.05, **P < 0.01, ***P < 0.001, unpaired two-tailed t test.

Fig. S13

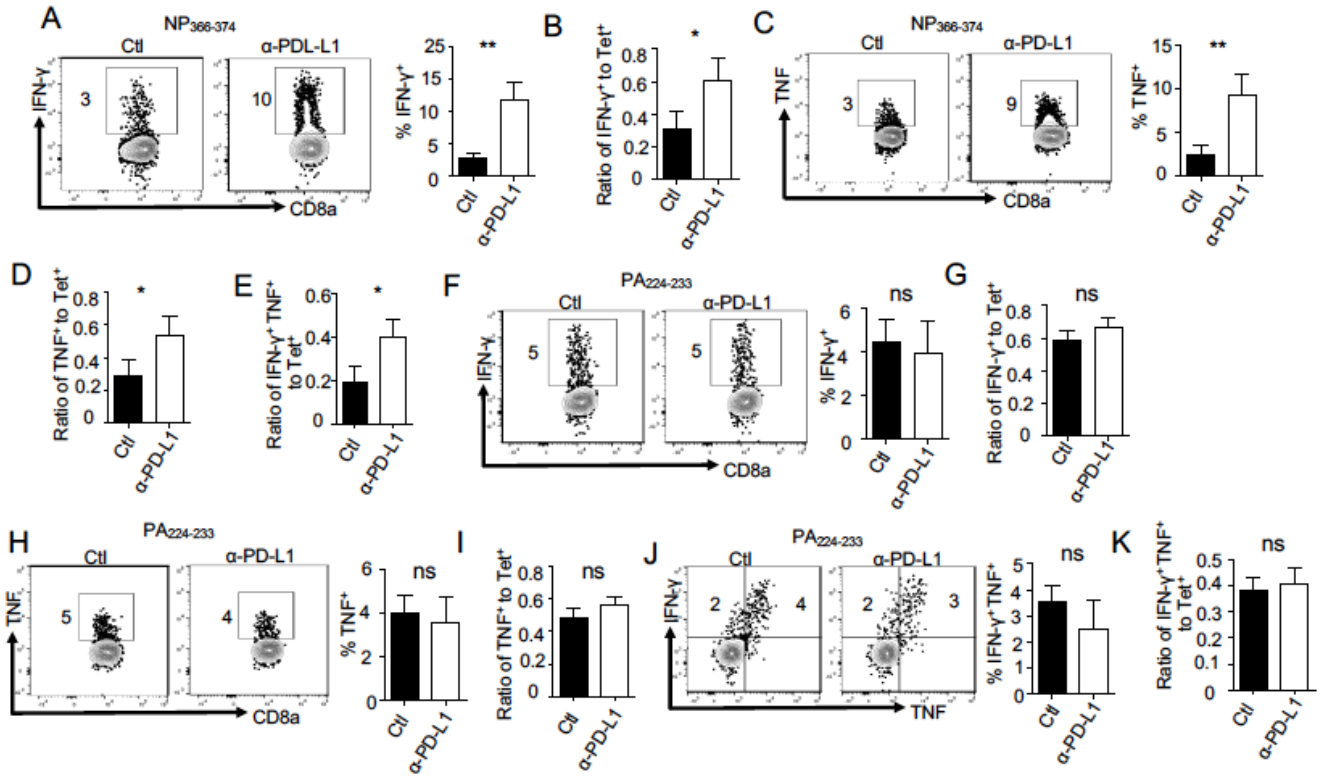

Fig. S13 PD-L1 blockade promotes cytokine production of exhausted-like T_{RM} cells to antigenic re-stimulation. (A-K). WT mice were infected with PR8 and treatment with control Ab or α-PD-L1 starting at day 21 p.i. Mice were sacrificed and lung cells were re-stimulated with $NP_{366-374}$ or $PA_{224-233}$ peptide *ex vivo* at 40 d.p.i. IFN-γ and TNF production by CD8 T cells following peptide restimulation were determined by ICS. (A). Representative plots (left) and quantification (right) of % IFN-γ$^+$ in resident-CD8 T cells following NP peptide stimulation. (B). Ratio of % IFN-γ$^+$ resident CD8 T cells cells following NP peptide stimulation to % $NP_{366-374}$ tetramer$^+$ in resident-CD8 T cells. (C). Representative plots (left) and quantification (right) of % TNF$^+$ in resident-CD8 T cells following NP peptide stimulation. (D). Ratio of % TNF$^+$ cells following NP peptide stimulation to % $NP_{366-374}$ tetramer$^+$ in resident-CD8 T cells. (E). Ratio of % IFN-γ$^+$ TNF$^+$ cells following NP peptide stimulation to % $NP_{366-374}$ tetramer$^+$ in resident-CD8 T cells. (F). Representative plots (left) and quantification (right) of % IFN-γ$^+$ in resident CD8 T cells following PA peptide stimulation. (G). Ratio of % IFN-γ$^+$ cells following PA peptide stimulation to % $PA_{224-233}$ tetramer$^+$ in resident-CD8 T cells. (H). Representative plots (left) and quantification (right) of % TNF$^+$ in resident-CD8 T cells following PA peptide stimulation. (I). Ratio of % TNF$^+$ cells following PA peptide stimulation to % $PA_{224-233}$ tet$^+$ in resident CD8 T cells. (J). Representative plots (left) and quantification (right) of IFN-γ$^+$ TNF$^+$ cells in resident-CD8 T cells following PA peptide stimulation. (K). Ratio of % IFN-γ$^+$ TNF$^+$ cells following PA peptide stimulation to % $PA_{224-233}$ tetramer$^+$ in resident CD8 T cells. Representative of three experiments. Data are mean ± SD, n.s., not significant. *P < 0.05, **P < 0.01, ***P < 0.001, unpaired two-tailed t test.

Fig. S14

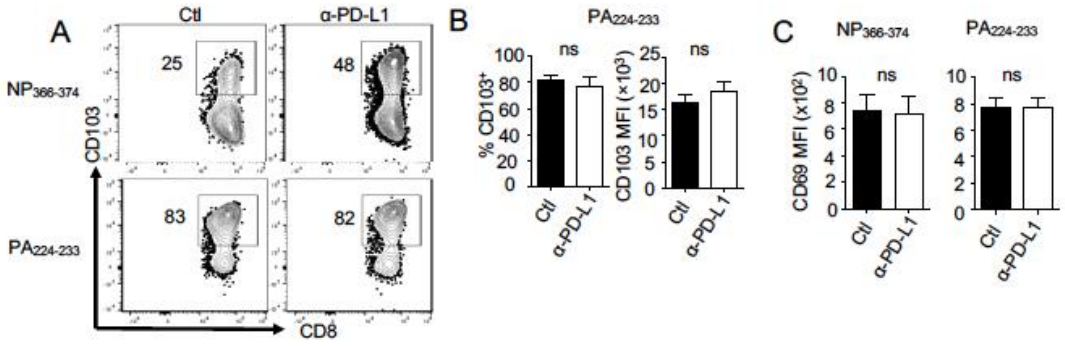

Fig. S14 PD-L1 blockade promotes CD103 expression. (A-C). WT mice were infected with PR8 and treated with control Ab or α-PD-L1 starting at day 21p.i. T_{RM} cells were analyzed at 40 d.p.i. (A). Representative plots of CD103 expression on $NP_{366-374}$ and $PA_{224-233}$ T_{RM} with or without late PD-L1 blockade. (B). Quantification of % $CD103^+$ cells (left) and CD103 MFI on (right) $PA_{224-233}$ T_{RM} with or without late PD-L1 blockade. (C). CD69 MFI on $NP_{366-374}$ or $PA_{224-233}$ T_{RM} with or without late PD-L1 blockade. Representative of three or five experiments. Data are mean ± SD, n.s, not significant. *P < 0.05, **P < 0.01, ***P < 0.001, unpaired two-tailed t test.

Fig. S15

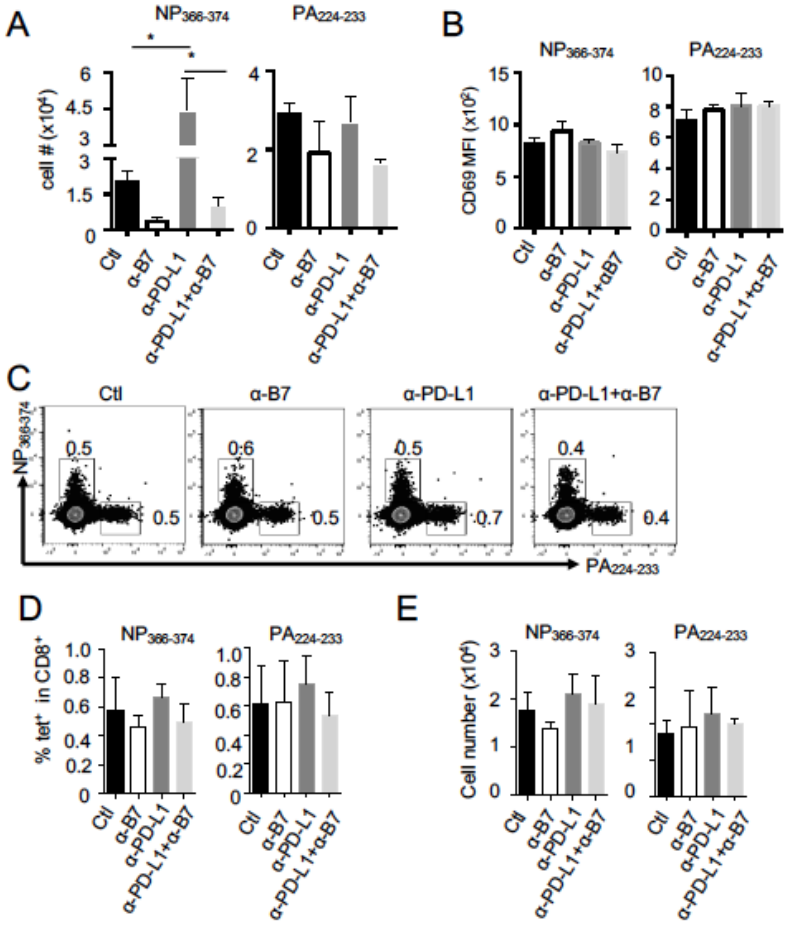

Fig. S15 B7 signaling is required for the effects of PD-L1 blockade. (A-E). WT mice were infected with PR8 and treated with control Ab, α-B7, α-PD-L1 or α-PD-L1 plus α-B7 starting at day 21p.i. T_{RM} cells were analyzed at 40 d.p.i. (A). Quantification of $NP_{366-374}$ or $PA_{224-233}$ T_{RM} cell numbers. (B). CD69 MFI of $NP_{366-374}$ or $PA_{224-233}$ T_{RM}. (C). Representative plots of % $NP_{366-374}$ or $PA_{224-233}$ cells in spleen CD8 T cells. (D). Quantification of % $NP_{366-374}$ or $PA_{224-233}$ cells in spleen CD8 T cells. (E). Quantification of $NP_{366-374}$ or $PA_{224-233}$ spleen memory T cell numbers. Representative of two experiments. Data are mean ± SD, *P < 0.05, **P < 0.01, ***P < 0.001, One-way ANOVA with Tukey multiple comparison test.

Fig. S16

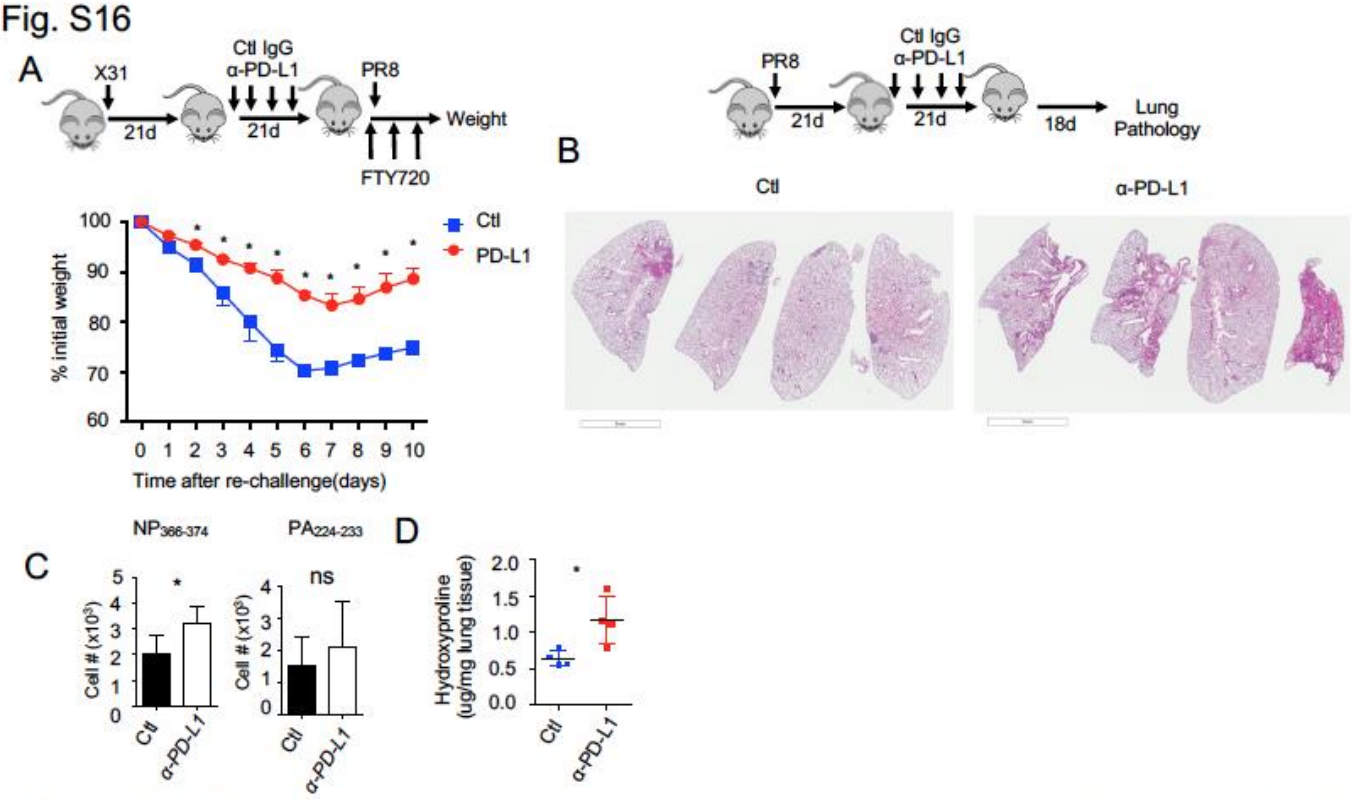

Fig. S16 PD-L1 blockade promotes heterologous immunity and causes tissue pathology. (A). WT mice were infected with X31. Control Ab or α-PD-L1 was administered starting at 21 d.p.i. as indicated. Mice were re-challenged with PR8 in the present of FTY-720 at 42 d.p.i. % of original weight was determined daily following re-challenge. (B). WT mice were infected with PR8 with or without PD-L1 blockade. Lung pathology was determined by H&E staining at 60 d.p.i. Low-magnitude picture of whole sections of lung left lobes from 4 individual mice are shown. Low-magnitude picture of whole sections of lung left lobes from 3-4 individual mice are shown. (C-D) WT mice were infected with PR8. Control Ab or α-PD-L1 was administered starting at 21 d.p.i. till 42 d.p.i. Mice were sacrificed at 90 d.p.i. (C). $NP_{366-374}$ or $PA_{224-233}$ T_{RM} numbers in the lung. (D). Lung collagen content was determined through hydroxyproline assay.

Fig. S17

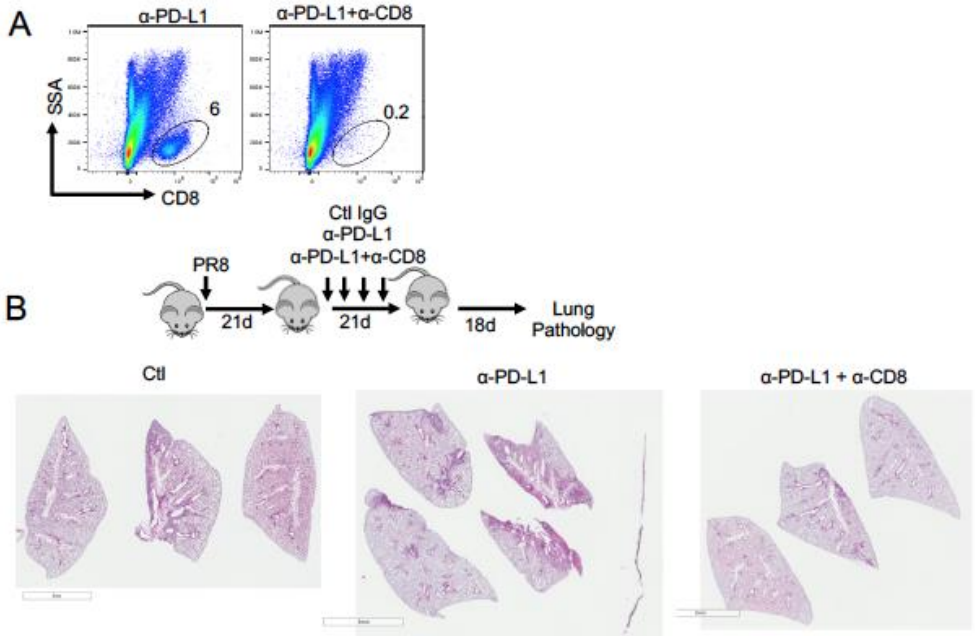

Fig. S17 CD8 T cells are responsible for the development of tissue pathology following α-PD-L1 blockade. WT mice were infected with PR8 and received control, PD-L1 or PD-L1 plus CD8 Abs. (A). Representative plots of lung CD8 T cells following α-PD-L1 or α-PD-L1 plus α-CD8 treatment at 60 d.p.i. (B). Lung pathology was determined by H&E staining at 60 d.p.i. Low-magnitude picture of whole sections of lung left lobes from 3-4 individual mice are shown.

Fig. S18

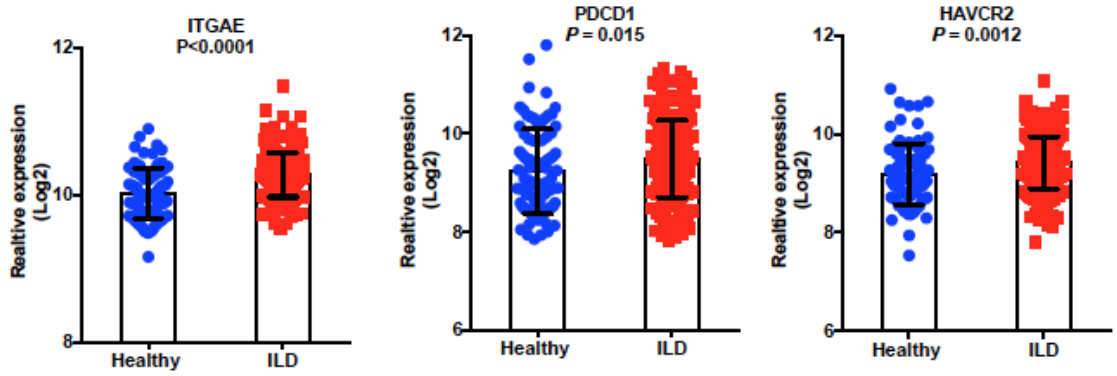

Fig. S18 ILD lungs exhibit elevated PD-1, CD103 and TIM-3 expression. ITGAE (CD103), PDCD1 (PD-1) and HAVCR2 (TIM-3) gene expression in publically-available microarray dataset (GSE47460) of lung biopsy samples from lungs of healthy or ILD patients. Unpaired two-tailed t test